Biological Structure and Dynamics, ISBN 0-940030-46-2
Proceedings of the Ninth Conversation, State University of New York. Albany, NY 1995
Eds. Ramaswamy H. Sarma and Mukti H. Sarma, ©Adenine Press 1996

On Low-Resolution Phasing of Neutron Diffraction Data Collected From Ribosomal Crystals

M. Roth[1], E. Pebay-Peyroula[1,2], A. Zaytzev-Bashan[3], N. Volkmann[4], Z. Berkovitch-Yellin[3,4], I. Agmon[3], F. Franceschi[5], A. Lewit-Bentley[6] and A. Yonath[3,4]*

[1]Struct. Biology Inst. J.P.Ebel, 41 Av. des Martyrs, 38027, Grenoble Cedex 1, France
[2]University J. Fourier, BP53X, 38041 Grenoble, France.
[3]Department of Structural Biology, Weizmann Institute, Rehovot, 76100, Israel
[4]Max-Planck-Lab. for Ribosomal Structure, Notke Str. 85, 22603, Hamburg, Germany
[5]Max-Planck-Inst. for Molecular Genetics, Ihne str. 73, 14159, Berlin, Germany

Abstract

Neutron diffraction data were collected to 30 Å resolution from crystals of the large ribosomal subunit from Haloarcula marismortui. Intending to match the solvent density with that of the ribosomal proteins or the ribosomal RNA, these crystals were immersed either in their normal or in a deuterated stabilization solution. Preliminary density maps were constructed from the observed neutron diffraction amplitudes, phased by direct methods. The main features of both maps were observed at approximately the same locations, but show different shapes. The map constructed from the data collected from the crystal kept at its regular stabilization solution, which should show mainly the ribosomal RNA, contains features which are comparable in size to that expected for the large ribosomal subunit, whereas that constructed at 100% D_2O is more fragmented. Superposition of these two maps on a map constructed from low-resolution X-ray data phased in a similar way showed similar packing motifs, thus provided preliminary information about the separation between the regions rich in rRNA and those rich in r-proteins which could be detected at the current resolution limits.

Introduction

Ribosomes are the universal cell organelles facilitating the translation of the genetic code into proteins. They are giant nucleoproteins, made of two subunits which associate upon the initiation of the translation process and dissociate at its termination. A typical bacterial ribosome contains more than a quarter of a million atoms and is of a molecular weight of 2.3 million daltons. It sediments with a coefficient of 70S. About two thirds of the ribosome is rRNA, composed of 3 chains of a total of about 4500 nucleotides. The other third contains r-proteins, the number of which depends on the bacterial source and varies

*Author to whom correspondence should be addressed. Phone: 49-40-89982802, Fax:49-40-891314E-mail: YONATH@MPGARS.DESY.DE

between 58 for eubacteria and 73 for the halophilic ribosomes. The large ribosomal subunit from Haloarcula marismortui, the subject of the studies presented here, is of molecular weight of 1.45 million daltons, contains two rRNA chains of more than 3000 nucleotides and over 42 proteins, the sequences of which are currently being determined (1).

For a better understanding of the molecular mechanism and the dynamical aspects of protein biosynthesis, molecular models are a prerequisite. To this end, X-ray and neutron crystallographic analysis are being carried out using crystals of functionally active, intact, modified or complexed ribosomal particles from halophilic and thermophilic bacteria (2), diffracting best to 2.9 Å resolution (3). The diffraction data of these crystals are either measured by X-rays at cryo temperature using intense synchrotron radiation facilities, or subjected to neutron diffraction studies at ambient temperatures.

Our X-ray crystallographic studies have been described elsewhere (e.g. 3-7). In this manuscript we present the current status of the neutron diffraction studies, using the crystals of the 50S subunits of H. marismortui (3), focusing on specific problems in data collection, evaluation and integration, and highlighting the structural results.

Neutron diffraction and the principles of contrast variation

Single crystal neutron diffraction combined with contrast variation is a technique which may facilitate the elucidation of selective structural elements (see, for instance, 8-14). It is based on the non-linear correspondence between the amplitude of the neutron scattering factors (F) and the atomic numbers (Z). Thus, atoms with similar atomic numbers may diffract neutrons according to very different scattering cross-sections. The most striking example is the hydrogen whose diffracting power is radically different from that of the deuterium. In structural studies on crystals of complex macromolecules, such as nucleoprotein assemblies, the different scaling lengths of the H and the D atoms is being exploited for matching the densities of the proteins or the nucleic acids with that of the solvent.

By varying the D_2O content in the crystal, the scattering length densities of the three crystal components (proteins, RNA and solvent) are changed, and therefore the contrast of the RNA and the proteins in respect to that of the solvent is modified (15). Depending on the resolution of the data and the level of intra-penetration of the two components, information about their internal distribution may be obtained.

At non-deuterated solutions the contrast between the rRNA and the solvent is higher than that of the proteins, whereas the situation is reversed for the proteins at 100% D_2O. Therefore the maps constructed from neutron diffraction data collected at these two extremes should be complementary. For equilibrating the crystals with the different deuterated solutions, they are soaked in the deuterated solutions of the desired compositions, and the diffraction is measured at a series of contrasts.

Since ribosomes are composed of two distinctly different chemical entities, r-proteins and rRNA, they should be appropriate candidates for such studies. The crystals of ribosomal particles, like most of the crystals of large biological molecules, contain large amounts of solvent. Thus, assuming that around 50% of the volume of the crystals of the ribosomal

subunits from H. marismortui is solvent, the volume fraction occupied by the rRNA and the r-proteins are estimated to be around 33% and 17% respectively. The solvent contributes significantly to the diffracted intensities, particularly at small angles of diffraction. This effect might considerably hamper attempts at low-resolution phasing, but at the same time may increase the chances for obtaining some structural information utilizing contrast-variation.

On the distribution of the rRNA and the proteins within the ribosome

Although more than two decades ago Sir F. Crick suggested that the original ribosome was made entirely of RNA, until recently it was assumed that the catalytic activities of the ribosome are carried out solely by proteins, and the rRNA molecules have a more passive role in transferring genetic information, or in providing the scaffold for the ribosome. Consequently, the common belief was that the RNA is concentrated mainly in the center of the particle, whereas most of the proteins are distributed on the surface. In many instances this hypothesis led to premature and somewhat misleading interpretations of results obtained by several biophysical methods, such as light scattering and electron microscopy, which because of their inherent nature tend to show apparent internal condensation of material. Thus, for over three decades ribosomal particles were reported as having a core of rRNA and a surface made of r-proteins (16-20).

However, the demonstration of the catalytic abilities of RNA in several biological systems, the accumulation of data showing substantial conservation in some rRNA regions, the possibility to target naturally exposed single strand rRNA regions by DNA oligomers, and the recent site-directed-mutagenesis experiments which uncovered specific roles, stimulated the design of experiments challenging the above dogma (21-28). These showed unequivocally that most of the ribosomal functions, such as the GTPase and the peptidyl transferase activities, are being carried out solely, or in part, by the ribosomal RNA, and therefore a substantial part of the RNA must be exposed on the surface and cannot be buried in the core of the ribosome.

Nevertheless, it is conceivable that part of the rRNA is clustered in distinct locations. Similarly, the observations that several r-proteins form in situ complexes in eubacteria (29), eukaryotes (30) and archeabacteria (1, 7, 31) indicate their partial clustering. Therefore it may be possible to determine the approximate locations of some of the ribosomal proteins and rRNA domains performing single crystal neutron diffraction experiments at different contrasts. Clearly, more detail is expected with the increase in resolution.

The collection of neutron diffraction data

Low-resolution neutron diffraction data were collected at the Institute Laue-Langevin (ILL, Grenoble, France) using the high flux reactor on DB21 diffractometer at 7.5 Å wavelength. Two data sets were recorded: the first from crystals containing hydrogenated solvent (called here 0% D_2O), the second from a crystal in which the labile hydrogen atoms of the solvent were exchanged by deuterium (called here 100% D_2O). For obtaining the latter, the crystal was soaked in a 100% deuterated solvent for three weeks in order

to deuterate most of the exchangeable hydrogens involved in N-H or O-H bonds within the ribosomal particle.

The main factor which determines the feasibility of neutron crystallography is the average intensity of the reflections. The signals obtained by the diffraction of neutrons are rather weak and dictate long measuring periods which are feasible because the neutron beam is not destructive. Thus, because of the relative small size of the ribosomal crystals and their large unit cell dimensions, for obtaining data to 30 Å resolution from the 100% D_2O crystals, they had to be exposed for three weeks. The situation at 0% D_2O was more acute, since under these conditions the signal to noise ratio is weaker due to the incoherent scattering from hydrogen atoms. Therefore five weeks were needed for the collection of a 40 Å resolution data set. The statistics of the diffraction data are summarized in table I.

Phase determination in ribosomal crystallography

Density maps, the basis for the determination of three-dimensional structures, are constructed by Fourier summation of the structure factors derived from the reflections which appear in the diffraction pattern. Each reflection is a wave characterized by its direction, amplitude and phase. The directions and amplitudes can be measured, whereas phases cannot be directly determined. Therefore the assignment of phases to the observed structure factor amplitude is the most crucial, albeit the most complicated and unpredictable step in structure determination, even when the object is an average-size protein. For ribosomal crystals, the magnitude and the complexity of this step is greatly enhanced.

Neutron diffraction studies are being performed either on unknown structures, in order to reveal the internal density distribution of multi components particles, using contrast variation, or on structures which have been determined crystallographically, in order to reveal features which cannot be otherwise studied, such as the locations of the hydrogen atoms or of detergent domains in membrane proteins. For the latter cases, the phase information is usually available from the X-ray measurements, whereas for the determination of the phases of unknown structures, procedures similar to those used in X-ray crystallography have to be employed.

Table I

Data statistics are given to a resolution of 30 Å. For computing data completeness, reflections with intensities larger then one and three sigmas were shown (the latter in brackets). Crystal symmetry: C2221. Unit cell constants: 214, 300, 580 Å (neutron data collected at ambient temperature) and 213, 300, 570+- 4 Å (X-rays data collected at cryo temperature).

Data statistics	100% D_2O	0% D_2O	X-ray
Total number of reflections	2021	1008	5892
Unique reflections	439	294	442
Rsym	10%	13%	5.4%
Completeness			
neutrons at 200-40 Å	94 (84)%	74 (44)%	
neutrons at 40-30 Å	86 (58)%	43 (15)%	
X-ray at 173-30 Å			85%

Isomorphous replacement is the most commonly used method for the determination of the phases of unknown structures of macromolecules by X-ray crystallography. It exploits the changes in the structure factor amplitudes caused by the addition of heavy atom compounds to the native crystals. The usage of this method requires almost

quantitative attachment of the heavy atoms at a limited number of sites within the unit cell, while keeping the crystal structure isomorphous to that of the native molecule. When only one derivative can be obtained, the Single Isomorphous Replacement (SIR) procedure, which yields ambiguous phasing, is used. More reliable phases are obtained when more than one heavy atom derivative is measured. Then the Multiple Isomorphous Replacement procedure (MIR) is being employed. For cases where the derivatized macromolecule contains a heavy atom which resonates with X-ray beam of a wavelength close to its absorption edge in a way which removes the symmetry between the reflections related by inversion, an alternative method, MAD (Multiple wave-length Anomalous Diffraction) is becoming increasingly fashionable. Providing the signal of the differences of the amplitudes of the corresponding terms can be determined accurately, a single derivative, exposed at several wavelengths may provide sufficient information for phase determination.

For proteins of average size, useful heavy atom derivatives consist of one or two heavy atoms. Clearly, because of the large size of the ribosome, compact and dense materials of a proportionally larger number of electrons, such as multi-metal salts (e.g. polyheteroanions or coordination compounds), or dense metal clusters (i.e. an undecagold) which can be directly bound to the particle prior to crystallization, should be more suitable. Most recently several such compounds were shown to be of adequate phasing power for preliminary low and intermediate resolution phasing of X-ray diffraction of ribosomal crystals (1, 7, 32).

The procedures for phase determination of the X-ray diffraction from crystals of small molecules are much simpler. Here the phases are routinely obtained by ab initio computational methods, exploiting the relationships between the dominant reflections (33). Naturally, a considerable effort has been devoted for the extension of these methods towards structure determination of macromolecules, especially for complicated systems, such as the ribosome, for which the suitability of the isomorphous replacement method was doubtful. Consequently, some of these approaches were extended and further developed for phasing the low-resolution data collected from ribosomal crystals (34). Several examples from the large range of approaches exploited in the context of low-resolution phasing of the ribosomal reflections are summarized below.

For suggesting the packing motifs and for detecting some envelope features of the large ribosomal subunit from Thermus thermophilus at about 80 Å resolution, entropy maximization with log-likelihood gain as a phase-set discriminator (35) was used (36, 37). The results of these studies were later supported by those obtained by the few-atom method (38) and by low-resolution molecular replacement studies (39), using the approximate model of this particle, which was obtained by three-dimensional image reconstruction from electron micrographs of tilt series of crystalline monolayers (40). The positions of the center-of-mass in the unit cell were also supported by the results of ultra low-resolution R-factor searches at various solvent contrasts (36, 41) and by the application of an extension of traditional direct methods combined with ellipsoidal modelling (42, 43). Molecular replacement studies with this model have also been performed on other crystal forms (44, 45). In addition, a new approach, combining elements of traditional direct methods, envelope refinement, maximum-entropy filtering, likelihood ranking, cross-val-

idation and cluster analysis, aiming at phasing at resolution up to 30 Å, is being developed (46). So far it has been applied to T50S and led to results that agree well with the previous ones (34).

Attempt at phasing the neutron diffraction data

While conducting the studies reported here, no phase information was available for the X-ray amplitudes collected from the crystals of H50S. Therefore an advanced version of the traditional Direct Methods (described in 34 and 42) was used for phasing at low-resolution. For selecting the most probable phase set, a new application was developed (42). This procedure was first tested on model cases and then applied to four different data sets independently collected from crystals of H50S: two sets of neutron diffraction data, collected from the crystals immersed in 100% and 0% D_2O, and two collected with X-rays from two native crystals. As the DM treated two X-ray diffraction sets led to almost the same center-of-mass positions, namely with a distance of 6 Å between them (43), only one was chosen for the comparative studies described below.

The first step in the phasing procedure is the location of the positions of the center-of-mass of the particles. For this step, the observed structure factors were normalized by spherical averaging (47). The so obtained E-normalized structure factors with an E values larger than 1 were phased by DM, using the program MITHRIL (48). A large number of phase sets were generated, of which the "best" was selected by a sorting procedure, based on specific statistical criteria (42), which score the differences between the E-values obtained by the E-normalization of the observed structure factors and the E-values calculated by representing the particle as an ideal point located at the center-of-mass, according to their R-factors, correlations, sum of least squares and packing considerations.

The center-of-mass is obtained by peak search in the E-map. For the three data sets, namely those collected by neutrons at 0% and 100% D_2O, as well as for those collected by X-rays from native crystals, the selected centers of mass were computed and refined against the low-resolution normalized observed structure factors. Table II shows the refined values of the coordinates of the centers of mass for the three cases. As seen, the x and z coordinates are rather similar in the three maps. The discrepancies between the values (maximum 32 Å) can be justified by the resolution limits of the data (40 Å).

Table II

The positions of the centers of mass and ellipsoid parameters for three independent maps constructed with phases determined by direct methods, using neutron diffraction data of crystals immersed in 0% and 100% D2O, and from *30 Å data collected by X-rays (43). For comparison, **the position determined from the Harker peaks in the X-ray E-Patterson map, are also listed.

Data set	Center-of-mass (Å)			Radii (Å)		
				x	Ry	Rz
Neutron 0% D_2O	62.0	18.9	97.1	63.6	82.6	89.9
Neutron 100% D_2O	75.2	15.2	90.1	69.7	98.5	67.0
X-ray data*	70.8	47.6	101.8	59.5	89.0	93.5
X-ray E-Patterson**	71	26	89			

The second step in the phasing procedure consists of phase refinement and modification. First, the phases of those very low-resolution structure factors, which were not determined by MITHRIL since the E-values of the reflections were smaller than 1, are calculated by assuming that the particle is reduced

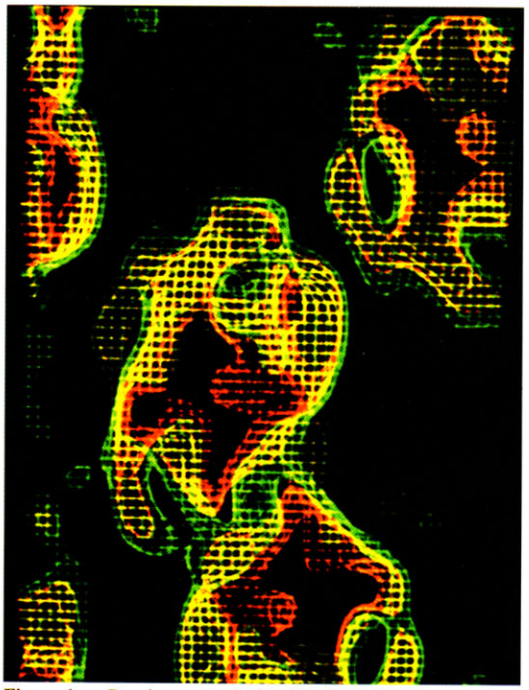

1a

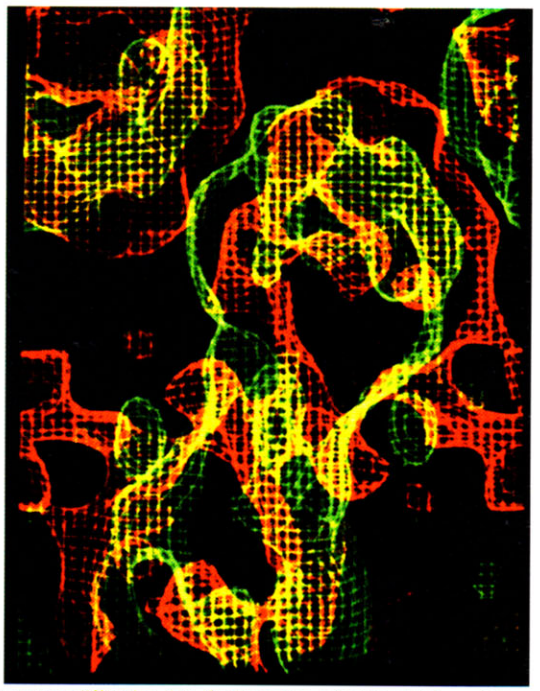

1b

Figure 1: a. Density map calculated by Fourier synthesis with the 0% D_2O neutron diffraction data. In the center, a feature which was interpreted as the ribosomal particle with its nearest neighbors, is clearly delineated with respect to the solvent. Two levels of density are shown. The lower contouring level was chosen to enclose 30% of the volume of the lattice (according to the following assumption: the volume of the entire particle corresponds to about 45-50% of the unit cell, and 2/3 of the particle is rRNA). This contour level corresponds to 0.5 sigma (i.e. 0.5 rms of the deviations of map density). As a consequence of the nature of the contrast at 0% D_2O, the features seen in this map should reveal the parts of the particle which are rich in rRNA.b. The superposition of two density maps. In green: resulting from the 0% D_2O neutron diffraction data. In red, that constructed from very low-resolution (173-27 Å) X-ray data, phased by DM, using the same procedure employed for the neutron sets. Despite the slight translation between the two centers, the gross shape similarities of these two images are evident.

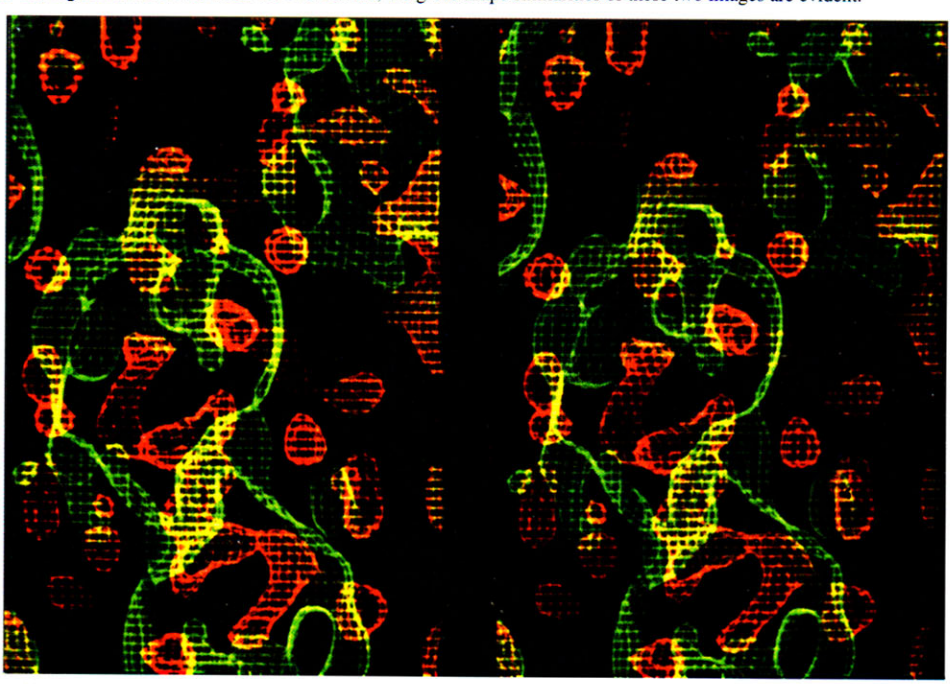

1c

c. Stereo view of the superposition of the two density maps. In green: the map constructed from the 0% D_2O neutron diffraction data. In red: the map constructed from the 100% D_2O neutron diffraction data. As explained above, at 100% D_2O the contrast between the r-proteins and the solvent is higher than that of the rRNA, whereas at 0% D_2O the contrast of the rRNA is the highest. The contour levels were chosen according to similar considerations taken for (a). However, as the 100% D_2O map is more noisy than that constructed from the 0% D_2O, to limit the contribution of noise to the features believed to represent the particle, the map was contoured at a level corresponding to 1.4 sigma (i.e. 1.4 rms of the deviations of the map density). The volume enclosed within the contoured regions was found to correspond to 10% of the unit cell, which is somewhat lower than the that expected for the proteins within the unit cell (15-17%).

to a point located at the position of the center-of-mass. Then, all phases are modified in order to take into account the influence of the particle form factor on the structure factors. At the present state of the development of this method, the form factor is calculated assuming the particle is an ellipsoid. The initial values of the ellipsoid parameters (mean radius and anisotropy along the crystallographic axes) were obtained from packing considerations and from the shape of the peak at the origin in the Patterson map (42). These values were refined using data up to 80 Å resolution, and phase modifications were then applied to phases up to 40 Å resolution. In the final stage the phases were refined and extended using the solvent flattening procedure (42).

Comparisons with other attempts at low-resolution phasing

It is noteworthy that the so obtained positions of the ND determined centers of mass are almost identical to that found in the 80 Å MIR phased data (7), to that derived from Harker sections of the E-Patterson X-ray map (49) and that obtained by ME combined with LAPS (34), a procedure which was also applied independently to an X-ray solvent contrast series (50). Furthermore, the Harker sections of the 0% D2O map overlapped with those found for the X-ray data, and although the E-Patterson map of the 100% D_2O is rather noisy, significant peaks could be found in similar locations, with the largest deviation of 25 Å between them.

In addition, the different phase sets were exposed to correlation comparisons, for which a reciprocal-space correlation function, which monitors the similarities within the phase sets (34), was used. For the 80 Å resolution data, a reasonable correlation was found between the phases calculated for the two neutron diffraction sets and those obtained for the X-ray data by maximum entropy (34). Thus, the highest correlations values are 69% and 44% for the 100% and 0% D_2O, respectively.

The preliminary neutron diffraction density maps

It was found that the structure factors extracted from the 0% and 100% D_2O 40 Å resolution data sets are not proportional to each other, therefore scaling between them reveals significant non-linear differences, indicating large density fluctuations inside the particles. It is conceivable that these fluctuations result from the coexistence of r-proteins and rRNA within the particle. This situation is somewhat analogous to isomorphous replacement experiments, as in both cases one deals with two isomorphous lattices containing "non-isomorphic" parts, resulting either from the addition of heavy atoms, or from the internal density fluctuations combined with changes in contrast with respect to the solvent.

The 40 Å 0% and 100% D_2O neutron diffraction density maps are shown in Fig. 1. As seen, both are relatively clean, and several dominant features could be identified in them. A thorough examination of the 0% D_2O map shows that its main feature is of a size which accords with that expected for this particle, thus may grossly indicate its envelope. As seen, this feature and its symmetry related ones are located in general positions, thus ruling out artefacts which may be enhanced by symmetry operations. The map constructed from the X-ray data with phases derived by the same phasing algorithm used for phasing the neutron data (43), shows significant similarity to that constructed from the neutron 0%

D_2O data (Fig. 1). This is not surprising since for both maps the highest contrast between the particle and the solvent is due to the rRNA, the major constituent of the ribosome.

The 100% D_2O density map which should show predominantly the locations of the ribosomal proteins is quite different from the 0% D_2O and the X-ray map, as instead of compact and rather continuous features, it shows a few isolated density regions distributed around common centers of mass, as expected.

The comparison of 0% and 100% D_2O maps reveals some complementarity between the density domains. Thus, several contacts between the two envelopes could be identified in some parts of the maps and density overlap in others (Fig. 1). In this way, locations for several separate internal domains of rRNA and of r-protein could be suggested, a result consistent with the fact that the isomorphous difference between the two contrasts was found to be as high as 72%. Since there is also some overlap between the features observed in the two maps, it is conceivable that besides the distinct rRNA and r-protein regions, most of the rRNA and the r-proteins are intricately mixed, so that their borders cannot be resolved at 40 Å resolution.

For further verification of the interpretation of the neutron diffraction maps, the model of the large ribosomal subunit from B. stearothermophilus, reconstructed from tilt series of negatively stained monolayers of this particle, viewed by electron microscopy (40) was successfully superimposed on the main feature of the 0% D_2O neutron map. The usage of the reconstructed images of ribosomal particles of one bacterial source together with the data obtained from crystals of ribosomal particles from other sources was based on the assumption that the gross structures of ribosomes from different sources are rather similar at low-resolution.

Even in our earlier studies, when only the 0% D_2O map was available, a careful investigation of this map enabled the detection of a tunnel in the halophilic 50S ribosomal subunit (44), similar to that found in the reconstructed model of the same subunit (40) and in the whole ribosome (51) from Bacillus stearothermophilus. The existence of an internal tunnel within the large ribosomal subunit was suggested more than two decades ago as a result of several biochemical experiments which showed that the ribosome masks the newly synthesized protein chains (52, 53). It was first observed in reconstructed images of 80S ribosomes packed in two-dimensional arrays, as a narrow elongated region of low density (54). More recent biochemical and structural experiments confirmed this assignment (reviewed in 2 and 55) and led to the production of improved crystals of complexes of ribosomes mimicking defined stages in protein biosynthesis (56) as well as the chemical studies, focused on the progression of nascent chains, the results of which could be modeled (57, 58).

Conclusions and prospects

In this article we have shown that low-resolution preliminary maps could be constructed from neutron diffraction data phased by direct methods. These maps may be partially interpreted by merging results from neutron diffraction contrast variation, X-ray crystallography, electron microscopy and image reconstruction.

Acknowledgement

The studies presented here have been initiated under the inspiration and guidance of the late Prof. H.G. Wittmann. We are grateful to all members of the groups working on ribosomal structure in Hamburg, Berlin and Rehovot, for illuminating discussions and for excellent experimental assistance, and to ILL (Grenoble), CHESS (Cornell) and EMBL/DESY (Hamburg) for letting us use their experimental stations.

Support was provided by the French-Israeli and French-German binational programs (AFIRST and DAAD/PROCOPE, respectively), the NIH (R01-GM34360), the Max-Planck-Society and the Kimmelman Center for Macromolecular Assembly at the Weizmann Institute. AY holds the Martin S. Kimmel Professorial Chair.

References and Footnotes

1. F. Franceschi, S. Weinstein, I. Sagi, M. Peretz, V. Weinrich, S. Morlang, K. Anagnostopoulos, N. Böddeker, M. Geva, I. Levin, I. Agmon, Z. Berkovitch-Yellin, T. Choli, P. Tsiboli, F. Schlünzen, H.A.S. Hansen, H. Bartels, W.S. Bennett, N. Volkmann, J. Thygesen, J. Harms, A. Zaytzev-Bashan, S. Krumbholz, R. Sharon, A. Dribin, E. Maltz and A. Yonath, in this volume (1995)
2. Z. Berkovitch-Yellin, W.S. Bennett and A. Yonath. In "Critical Reviews in Biochemistry and Molecular Biology" Vol. 27, 403 (1992)
3. K. von Böhlen, I. Makowski, H.A.S. Hansen, H. Bartels, Z. Berkovitch-Yellin, A. Zaytzev- Bashan, S. Meyer, C. Paulke, F. Franceschi and A. Yonath, *J. Mol. Biol. 222*, 11 (1991)
4. Z. Berkovitch-Yellin, H.A.S. Hansen, S. Weinstein, M. Eisenstein, K.von Böhlen, I. Agmon, U. Evers, J. Thygesen, N. Volkmann, H. Bartels, F. Schlünzen, A. Zaytzev- Bashan, R. Sharon, I. Levine, A. Dribin, G. Kryger, W.S. Bennett, F. Franceschi & A. Yonath. In *Synchrotron Radiation in Biosciences* (B. Chance et al., Eds.) Clarendon Press, pp. 61 (1994)
5. J. Harms, F. Schlünzen, K. von Böhlen, J. Thygesen, S. Meyer, I. Dunkel, B. Donzelmann, H.A.S. Hansen, A. Zaytzev-Bashan, A. Dribin, G. Kryger, G. Thoms, N. Volkmann, H. Bartels, W.S. Bennett and A.Yonath. *ESF Report* (K. Wilson Ed.) pp. 26 (1993)
6. I. Agmon, H. Bartels, A. Bashan, W.S. Bennett, Z. Berkovitch-Yellin, N. Böddeker, A. Dribin, M. Eisenstein, F. Franceschi, H.A.S. Hansen, J. Harms, W. Jahn, S. Krumbholz, I. Levin, M. Malemud, S. Morlang, M. Peretz, I. Sagi, F. Schlünzen, R. Sharon, J. Thygesen, N. Volkmann, V. Weinrich, S. Weinstein and A. Yonath. In "Supramolecular Structure" (G. Pifat, ed.) in the press (1995)
7. F. Schlünzen, H.A.S. Hansen, J. Thygesen, W.S. Bennett, N. Volkmann, I. Levin, J. Harms, H. Bartels, A. Zaytzev-Bashan, Z. Berkovitch-Yellin, I. Sagi, F. Franceschi, S. Krumbholz, M. Geva, S. Weinstein, I. Agmon, N. Böddeker, S. Morlang, R. Sharon, A. Dribin, E. Maltz, M. Peretz, V. Weinrich, and A. Yonath, *J. of Biochemistry and Cell Biology*, in the press (1995)
8. L. Bragg and M.F. Perutz, *Acta Cryst. 5*, 277 (1952)
9. V. Luzatti, A. Tardieu, L. Mateu and H.B. Stuhrmann. *J.Mol. Biol. 101*, 115 (1976)
10. G.A. Bentley, J.T. Finch, A. Lewit-Bentley. *J. Mol. Biol. 145*, 771 (1981)
11. G.A. Bentley, A. Lewit-Bentley, J.T. Finch, A. Podjarny and M. Roth. *J. Mol. Biol. 148*, 55 (1984)
12. M. Roth, A. Lewit-Bentley and G. Bentley. *J. Applied Crystallography, 17*, 77 (1984)
13. Roth, A. Arnoux B., Ducruix, A. and Reiss-Husson, F. *J. Biochemistry, 30*, 9403 (1991)
14. C.V. Carter jr, K.V. Crumley, D.E. Coleman, F. Hage, *Acta Cryst A46*, 57 (1990)
15. B. Jacrot. *Rep. Prog. Phys., 39*, 911 (1976)
16. W. Kuhlbrandt and P.N.T. Unwin, *J. Mol. Biol., 156*, 611 (1982)
17. J. Frank, P. Penczek, R. Grassucci and S.J. Srivastava, *Cell Biol. 115*, 597, (1991)
18. R.P. May, V. Nowotny, P. Nowotny, H. Voss and K.N. Nierhaus. *Embo J. 11*, 373 (1992)
19. D.I. Svergun, M.H.J. Koch and I.M. Serdyuk, *J. Mol. Biol. 240*, 66 (1994)
20. D.I. Svergun, M.H.J. Koch, J. Skov Pedersen and I.N. Serdyuk, *J. Mol. Biol. 240*, 78 (1994)
21. P.C. Ryan, M. Lu, D.E. Draper, *J. Mol. Biol. 221*, 1257 (1991)
22. H.F. Noller. *Ann. Rev. Biochem. 60*, 191 (1991)
23. H.F. Noller, V. Hoffarth and L. Zimniak, *Science, 256*, 1461 (1991)
24. J. Ciesiolka, S. Lorenz and V.A. Erdmann. *Eur. J. Biochem, 204*, 575 (1992)

25. C. Brunel, P. Romby, E. Westhof, C. Ehrshmann and B. Ehresmann, *J. Mol. Biol., 221*, 293 (1991)
26. L. de Stevenson, P. Romby, F. Baudin, C. Brunal, E. Westhof, C. Ehrshmann, B. Ehresmann and P.J. Romaniuk, *J. Mol. Biol. 219*, 243 (1991)
27. G. Schreiber, S. Metzger, E. Azinman, S. Roza, M. Cashel and G. Glaser, *J. Biol. Chem. 266*, 3760 (1992)
28. A. Yonath and F. Franceschi, *Current Opinion in Structural Biology, 3*, 45 (1993)
29. W. Moller and J.A. Maasen, in: *On the Structure, Function and Genetics of Ribosomes*, (B. Hardesty and G. Kramer, Eds) Springer Verlag, NY, pp. 309 (1986)
30. M.T. Sean's-Robles, M.D. Villela, G. Pucciarelli, F. Polo, M. Remacha, B.L. Ortiz, F.J. Vidales and J.P.G. Ballesta. Eur. *J. Biochem. 177*, 531 (1988)
31. C. Casiano, A.T. Matheson and R.R. Traut, *J. Biol. Chem. 265*, 18757 (1990)
32. H. Bartels, W.S. Bennett, H.A.S. Hansen, M. Eisenstein, S. Weinstein, J. Müssig, N. Volkmann, F. Schlünzen, I. Agmon, F. Franceschi and A. Yonath. *J. Peptide Sciences*, in the press (1995)
33. Giacovazzo, C. *Direct Methods in Crystallography*, Academic Press, London. (1980)
34. N. Volkmann, F. Schlünzen, E.A. Vernoslava, A.G. Urzhumstev, A.D. Podjarny, M. Roth, E. Pebay-Peyroula, Z. Berkovitch-Yellin, A. Zaytzev-Bashan and A. Yonath. Joint *CCP4* and *ESF-EACBM Newsletters*, pp. 25, June (1995)
35. G. Bricogne, *Acta Crys. A40*, 410 (1984)
36. N. Volkmann. 1993. *Ph. D. Thesis*. University of Hamburg, Germany (1993)
37. N. Volkmann. In: *Entropy, Likelihood, Baysian Inference and their Application in Crystal Structure Determination*, Edited by G. Bricogne, American Cryst. Assoc. in the press (1995)
38. V.Y. Lunin, N.M. Lunina, T.E. Petrova, E.A., Vernoslava, A.G. Urzhumstev and A.D. Podjarny. *Acta Cryst. D51*. In the press (1995)
39. A.G. Urzhumstev and A.D. Podjarny, *Acta Cryst. D51*. In the press (1995)
40. A. Yonath, K.R. Leonard and H.G. Wittmann, *Science, 236*, 813 (1987)
41. F. Schlünzen, *Ph.D. Thesis*, U. of Hamburg, Germany (1994)
42. M. Roth and E. Pebay-Peyroula. In: *Entropy, Likelihood, Baysian Inference and their Application in Crystal Structure Determination*, Edited by G. Bricogne, American Cryst. Assoc. in the press (1995)
43. A. Zaytzev-Bashan, *Ph.D. Thesis*. Weizmann Inst. Rehovot, Israel (1995)
44. Z. Berkovitch-Yellin, H.G. Wittmann and A. Yonath, *Acta Crystallography B46*, 637 (1990).
45. M. Eisenstein, R. Sharon, Z. Berkovitch-Yellin, H.S. Gewitz, S. Weinstein, E. Pebay-Peyroula, M. Roth and A. Yonath. *Biochemie, 73*, 897 (1991)
46. N. Volkmann, in preparation
47. M. Roth. In: *Crystallographic Computing* (Eds. Moras Podjarny and Thierry), pp. 229 (1990)
48. C. J. Gilmore. *J. Appl. Cryst., 17*, 42 (1984)
49. I. Agmon and E. Pebay-Peyroula. To be published
50. N. Volkmann, H.A.S. Hansen, F. Schlünzen, A. Zaytzev-Bashan and A. Yonath, in preparation.
51. T. Arad, J. Piefke, S. Weinstein, H.S. Gewitz, A. Yonath and H.G. Wittmann, *Biochimie, 69*, 1001, (1987)
52. L.I. Malkin and A. Rich, *J. Mol. Biol., 26*, 329 (1967)
53. G. Blobel and D.D. Sabatini, *J. Cell Biol., 45*, 130 (1970)
54. R.A. Milligan and P.N.T. Unwin, *Nature, 319*, 693 (1986)
55. A. Yonath and Z. Berkovitch-Yellin, *Current Opinion in Structural Biology, 3*, 175 (1993)
56. H.A.S. Hansen, N. Volkmann, J. Piefke, C. Glotz, S. Weinstein, I. Makowski, S. Meyer, H.G. Wittmann and A. Yonath. *Biochem. Biophys. Acta 1050*, 1 (1990)
57. M. Eisenstein, B. Hardesty, O.W. Odom, W. Kudlicki, G. Kramer, T. Arad, F. Franceschi & A. Yonath. In: *Biophysical Methods in Molecular Biology* (G. Pifat Ed.) Balaban Press, Rehovot, pp. 213 (1994)
58. B.A. Hardesty, A. Yonath, G. Kramer, O.W. Odom, M. Eisenstein, F. Franceschi and W. Kudlicki. In: *Membrane Protein Transport* (S.S. Rothman, Ed.), in the press (1994)